Modeling surface velocities in the Southern and Eastern Alps by finite dislocations at crustal depths

A. Caporali
University of Padova, Department of Geosciences, Italy

G. Stangl
Austrian Academy of Sciences and Bundesamt fuer Eich – und Vermessungswesen, Austria

Abstract

The indentation of the Adria plate into the Southern – Eastern Alps is an ongoing collisional process accompanied by seismicity, uplift and lateral escape. We attempt a first 3D quantitative description of the process by combining GPS and structural data with an elastic dislocation model. GPS horizontal velocities of 75 Austrian and Italian permanent stations in the Eastern and Southern Alps serve as boundary condition on the free surface of an elastic half space containing six rectangular faults, each with an uniform, frictionless slip rate. Using the Okada (1985) algorithm, and taking into account the structural setting of the area and the geographic distribution of the velocity data, the geometry of the rectangular faults, the slip rate and its rake are constrained by least squares. We find that the surface velocities of the order of some mm/yr require slips at crustal depth ranging for 1 to 5 cm/yr, with rake mostly reverse, occasionally transpressional. The horizontal gradient of the moment (or potency) rate, rather than the moment rate itself, associated to each rectangular fault positively correlates with seismicity. The regional stress pattern computed from fault plane solutions agrees very well with the principal directions of our rectangular fault planes. The model, although constrained by horizontal velocities only, predicts a pattern of vertical motion which qualitatively agrees with known phenomena such as the uplift in the Tauern or subsidence in the Po Plain. Our results imply, more generally, that at or near deformable margins the convergence rate at the surface is considerably smaller than at depth, whereas for a rigid indenter the convergence rate is depth independent.

1 Introduction

In the Eastern and Southern Alps there is a complex fault geometry accommodating the Northwards indentation of the Adria plate, the uplift of the Tauern window and lateral extrusion towards the Pannonian Basin. The NorthEastern edge of the Adria is associated with the seismically active Friuli (Anderson and Jackson, 1987; Bressan et al., 1998,2006; Schmid et al., 2004, 2008), the compressive M_w=6.5 earthquake of May 6, 1976 being the largest recorded event. The area of the Southern and Eastern Alps is characterized by significant crustal thickness variations (Brueckl at al., 2007, 2010). Seismic profiles show that the Eurasian and Adriatic plates interact with a thinner Pannonian unit as a structurally separated entity. Late Oligocene–Middle Miocene indentation tectonics is considered as the primary agent driving substantial lateral material transfer, or "lateral extrusion" (Ratschbacher et al.,1991; Neubauer et al., 2000). Analog experiments (Regenauer-Lieb and Petit, 1997) have shown that the deformation resulting from the indentation of the rigid Adria into a plastic Eurasia depends on the ratio of the width of the indenter and the horizontal extent of the deformable foreland in the direction of the indentation. These analog experiments have shed light on the way the Alpine collision cuts the European lithosphere and is therefore linked to intraplate grabens.

Little is known about the present day processes shaping the Eastern and Southern Alps. For example, it is unclear if the Late Miocene–Recent horizontal and vertical motions in the Alpine Dinaric region are controlled by deep lithospheric, post glacial isostatic adjustment or surface/climatic processes. Another open question is how do NW-striking dextral fault systems in the Alpine Dinaric region (example: the Lavanttal and Drava- Moelltal fault systems to the East, and the Schio Vicenza line to the West) kinematically link with East striking thrust faults in Friuli (example: Pustertal–Gailtal fault segments of the Periadriatic Line), and the leftlateral Salzachtal-Ennstal–Mariazell–Puchberg (SEMP) fault), and how is that kinematic transition topographically expressed (Fig. 1).

There is seismological, geologic and geodetic indication of the existence of a triple junction East of the Tauern Window, joining the European, Adria and a thin Pannonian unit (Brueckl et al., 2007, 2010). According to the palinspastic reconstruction by Linzer et al. (2002), the average velocity of extrusion East of the Tauern Window was 5 to 6 mm/yr during the most active phase in the Oligocene and Miocene. However geodetic data show that recent extrusion occurs at much lower velocities of only about 1 mm/yr (Grenerczy and Kenyeres, 2006; Weber et al., 2006; Caporali et al., 2009). How much slip, if any, is involved along the Pustertal Gailtal (Periadriatic) and the SEMP lines is still a subject of discussion.
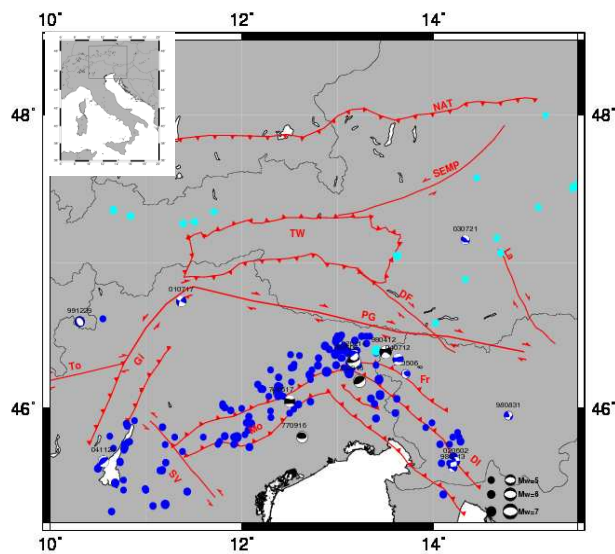

Fig. 1. Large scale fault structure in the Eastern-Southern Alps and recent seismicity. To = Tonale line, PG = Pustertal-Gailtal, Gi = Giudicarie Line, TW = Tauern Window, NAT = North Adriatic Thrust, La = Lavant Fault, DF = Drava Moelltal Fault, Di = Dinarides, Mo = Montello, Fr = Friuli, SEMP = Salzachtal-Ennstal–Mariazell–Puchberg fault. Vergence and faults stile are from the Structural Model of Italy (CNR, 1990). CMT mechanisms of events from 1976 to 1999 (black compression) are from the Harvard CMT Catalogue. Later CMT solutions (blue compression) are from the Regional Catalogue of Pondrelli et al. (2011). The events are labeled by their date in the format yymmdd. Historic events are taken from the CPTI04 Catalogue (blue solid dots: Gruppo di Lavoro CPTI04, 2008) and from the ZAMG Catalogue (http://www.zamg.ac.at/forschung/geophysik/erdbeben forschung/: light blue solid dots).

According to the lateral extrusion model (TRANSALP Working Group, 2002; Castellarin et al., 2006), thrusting up the Subtauern ramp has been a major component of the exhumation of the Tauern. A convergence of 3 mm/yr is expected to result in an uplift rate smaller than 1 mm/yr. According to Barletta et al. (2006), such value could be significantly increased by the post glacial rebound or the effect of recent glacier melting. By contrast, there is little or no knowledge on the amount of present day strike slip on the lateral fault systems, such as the Schio Vicenza and Giudicarie on the W (Massironi et al., 2006) and the Upper Dinarids to the E (Carulli et al., 1990). Here the present day seismicity is lower than in the Friuli region, which contains the tip of the indenter. In the neighborhood of the Drava Fault at least two events of M=6.1 have occurred, in 1201 and 1690, according to the historical Catalogue at the Austrian Zentral Anstalt fuer Meteorologie und Geodynamik (http://www.zamg.ac.at/forschung/geophysik/erdbeben forschung/) . On the Northern edge of the Giudicarie line a sinistral strike slip earthquake of Mw=4.9 occurred in 2001 near the town of Merano (Caporali et al., 2005).

According to recent paleomagnetic data, the Adria microplate can be considered a separate structure from the Nubia plate (Battaglia et al., 2004; Marton et al., 2011). The departures from rigidity of the crust at or near plate boundaries cause specific patterns in the velocities of GNSS stations in these areas and provide a boundary condition for the deformation at depth. Faults and slip rates have been mapped and are described in detail in the Database of individual Seismogenic Sources (Basili et al., 2008) along the Friuli and Montello lines. Detailed profiles in the NS and EW directions have been published on the basis of dense GPS velocity solutions (D'Agostino et al., 2006,2008; Caporali et al., 2009), but we do not know about the present day causative slip at depth. It is then natural to ask if such patterns of superficial horizontal velocities could be due to slip on a limited number of rectangular faults, what would be their geometry (position, orientation, size) and amount of slip, and the relation of such faults to the tectonic structure of the area, resulting from seismology and structural geology.

Using the analytic model of finite dislocation in an elastic half space of Okada (1985), we present in this paper a first attempt to map frictionless slip at depth. Using structural geology data we identify a number of rectangular faults which approximate the largest geological structures and which have the potential to accommodate the slip required to fit the GPS data. We show that the GPS velocities, of the order of a few

mm/yr, are consistent with a dynamic process where indentation and lateral extrusion involve slips at crustal depths ranging between 10 and 50 mm/yr. The available velocity data enable us to identify six rectangular patches where slip takes place, and associate them with the Giudicarie line, the Southern border of the Tauern Window, the North Alpine Thrust, the Drava-Moelltal fault and the two segments of the Montello – Friuli fault. Using the root mean square (r.m.s.) of the (observed-minus-modeled) velocities as an indicator of the goodness of the fit, we constrain the geometries of the rectangular faults and slip rates.

2 Data, Method of Analysis and Accuracy

We used velocities data resulting from the multi-year cumulative solutions done at the Austrian Academy of Sciences in Graz and at the University of Padova. Both are active as EUREF Analysis Centers and use the processing standards recommended by the International GNSS Service and the European Permanent Network of EUREF (http://www.epncb.oma.be/_organisation/guidelines/guidelines_analysis_centres.pdf) and Bernese Software (Dach et al., 2006). The common processing strategies and a common frame for position and velocities are such that the velocities from the different solutions to form one homogenous set. Small discrepancies may exist due to the different time span, for example, but these are typically smaller than 0.5 mm/yr and have a negligible impact on the final interpretation . The estimated velocities are shown on Fig.2. All the velocities were computed in ITRF2005 (Altamimi et al., 2007) and reduced to an Eurasian reference frame with the same Euler rotation vector. Formal error ellipses have been rescaled to account for colored noise in the coordinate time series (Caporali, 2003). There are, in a broad sense, three distinct patterns of velocities.
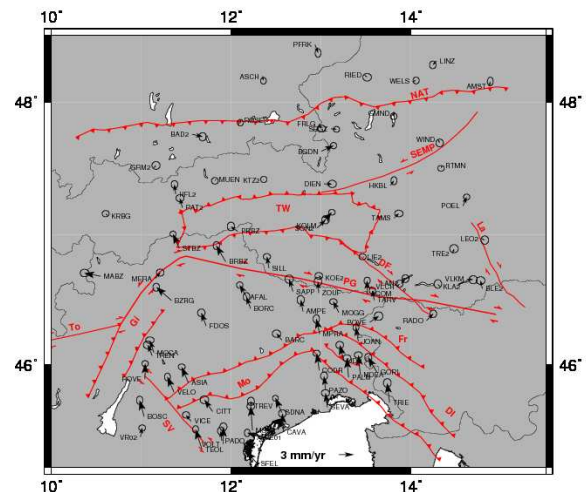

Fig. 2. The geographical distribution of the GPS velocities used in this study.

On the southern part (South of TW) there is a dominant Northwards component, indicative of the ongoing indentation on the Adria plate. There is a growing NW component in the Western part of the figure, in very good agreement with the direction of the most compressional axis of the stress tensor resulting from the inversion of seismological events (see Fig.10 in Bressan et al., 1998). On the Northern part, North of NAT, the velocities are smaller in size and heading south. On the center- East part of the plot, between NAT and TW, there is a marked component in the East direction, as already noted (Weber et al., 2006; Grenerczy and Kenyeres, 2006; Caporali et al., 2009), suggesting that an Eastward motion is still active at present (Brueckl et al., 2010).

To estimate which displacements at depth are associated to the observed surface velocities, we use the Okada (1985) model of displacement of an elastic half space, in terms of uniform, frictionless slip on a rectangular fault. The extension of the considered area and the spatial resolution of the available velocity data suggest that several rectangular faults need to be introduced. The model velocities on the surface are the vector sum of the displacements associated to each
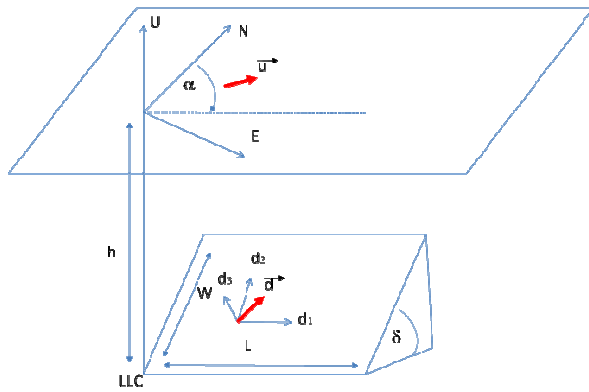
fault.

Fig. 3. The geometry of the Okada model of dislocation in an elastic half space, relating the displacement _u_ measured at the surface by GPS geodesy to the slip _d_ at depth, constant on the rectangular patch. The origin of the coordinates corresponds to the Lower Left Corner (LLC) of the rectangular patch. The N, E, U directions define the local reference system at the surface (North, East, Up).

A total of nine independent parameters need to be specified for each rectangular fault (Fig.3): the position (latitude/longitude/depth) of the lower left corner (LLC) of the rectangle; the strike α and dip δ angles; the length L and width W of the rectangle and the two dimensional slip vector $(d_1,d_2,0)$ of the hanging wall relative to the foot wall. We assume $d_3=0$. The ratio of the P and S velocities of seismic waves was fixed to Vp/Vs=1.89.The knowledge of the large scale structural setting of the area provides guidance to nominal values for all the parameters, except for the slip vector _d_. We set to six the maximum number of rectangular faults for our model, based on the consideration that each rectangular fault has nine free parameters. We use horizontal velocities of 75 sites, hence 150 observations, so that six rectangles will leave us with 96 degrees of.freedom. Relying on large scale structures is therefore necessary, given the number and geographical distribution of the available data. We tested several hypotheses of rectangular faults, based upon the regional fault structure. We eliminated those rectangular faults which had no influence on the total r.m.s.. We also tried to lump together smaller rectangular faults, to minimize the number of adjustable parameters.
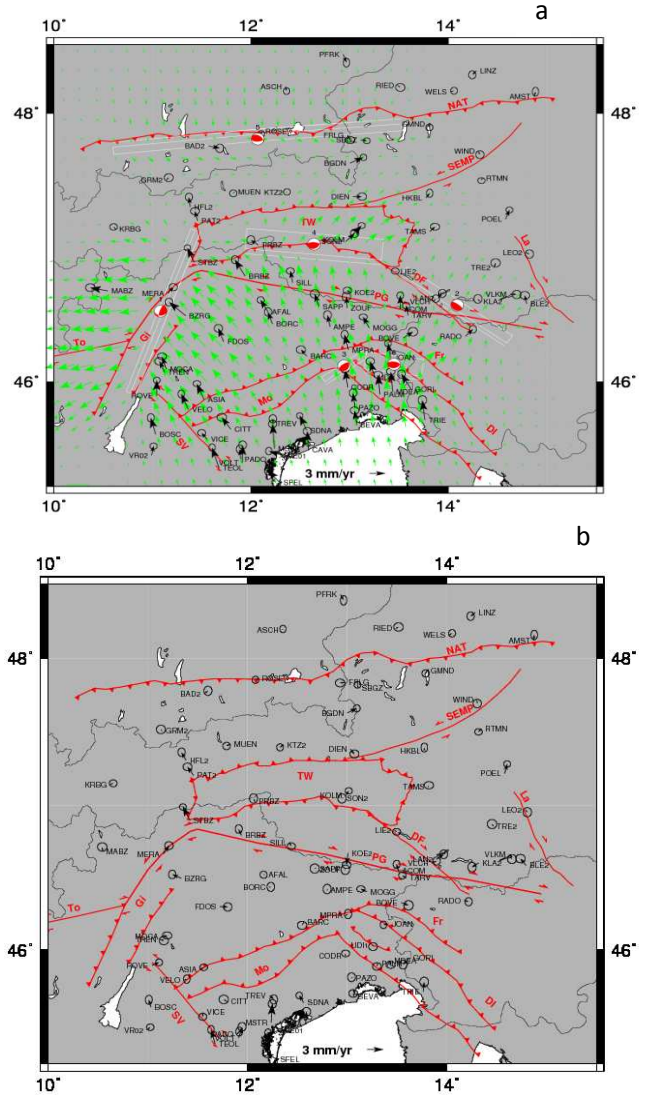

Fig. 4.(a) geometry of the six rectangular patches (grey rectangles) projected to the topographic surface. The grey line parallel to one of the sides of each rectangle represents the intersection of the fault plane with the topographic surface. The 'beach balls' give a pictorial view of the data in Table 2. The number in black above each beach ball refers to the indexing in Table 2. The green arrows represent the prediction of the model on a regular grid. (b) residual velocities (observed – computed), showing the likelihood of the model to represent the data, within the estimated uncertainties at each site

For example, the Giudicarie line was initially resolved into two separate segments, but tests showed that one

large scale structure was sufficient. A similar attempt was done for the Friuli and Montello rectangular faults.

In this case it turned out that the two needed to be separate. We then computed numerically partial derivatives of the horizontal velocities relative to the fault parameters and estimated final least squares corrections, and the formal uncertainties. Figure 4a shows the six rectangular faults that are needed to generate model velocities with a r.m.s. of 0.95 mm/yr, and the surface velocities predicted by the model, interpolated to a regular grid, to highlight the predicted surface kinematics. Figure 4b shows the residual velocities e, in the sense of measured velocity – minus – computed velocity. The residual velocities are in most cases smaller than their uncertainty, providing an indication of the goodness of the model. Table 2 gives the best fitting nine parameters for each of the six rectangular faults. The last column contains as a derived information the 'potency rate', that is the product of the slip area times the slip rate, scaled by the shear modulus μ=30 GPa. This quantity can be considered a moment rate.

Table 1. The nine parameters of each of the six rectangular faults used in the analysis, and their estimated formal uncertainty, in the sense of square root of the corresponding element in the variance covariance matrix scaled by the r.m.s. of the post fit residuals. The last column gives the product of the previous three columns (slip area x slip rate) times the shear modulus μ = 30 GPa.

id#	Structural element	Lon (deg)	Lat (deg)	Depth (km)	Strike (deg)	Dip (deg)	Slip (deg)	Dislocation (m)	Length (km)	Width (km)	In plane moment rate (10^{18} J/yr)
1	Giudicarie	11.39	47.15	45	200	80	60	0.050	145	20	4.35
		±0.17	±0.11	±25	±5	±8	±6	±0.067	±22	±30	
2	Drava Moelltal	14.65	46.35	40	305	75	90	0.010	100	30	0.90
		±0.26	0±.18	±9	±13	±17	±15	±0.004	±42	±9	
3	Montello	13.14	46.24	15	235	65	100	0.010	40	10	0.12
		±0.42	±0.25	±13	±3	±35	±37	±0.025	±25	±21	
4	Tauern	13.34	47.07	45	275	65	110	0.015	105	40	1.89
		±0.21	±0.09	±9	±7	±8	±8	±0.006	±24	±14	
5	North Adriatic Thrust	10.61	47.70	14	85	55	65	0.010	220	10	0.66
		±0.39	±0.06	±5	±5	±17	±22	±0.001	±95	±5	
6	Friuli	13.75	46.17	25	278	55	100	0.020	45	25	0.68
		±0.17	±0.09	±6	±11	±6	±12	±0.01	±20	±8	

Figures 5 and 6 provide a 3D view from West and South respectively of the rectangular faults constrained by the data, and the direction of slip of the hanging wall relative to the footwalls.

3 Discussion

We have investigated the hypothesis that the indentation of Adria into the Eastern Southern Alps, and related phenomena such as uplift and lateral extrusion, can be modeled in terms of dislocation of an elastic half space. Frictionless slip on a finite number of rectangular faults maps into displacement on the free surface of the half space, which is compared with the horizontal velocities of GPS stations. The location, size and orientation of the rectangular faults are close to those of regional tectonic lineaments, which exhibit a variable degree of seismicity. The deformation pattern requires the indenter to be non rigid. Adria deforms considerably in the contact zone with large scale structures, and the deformation can be modeled locally, i.e. without invoking the thrust generated on the Adria plate by the push of the Nubia plate.
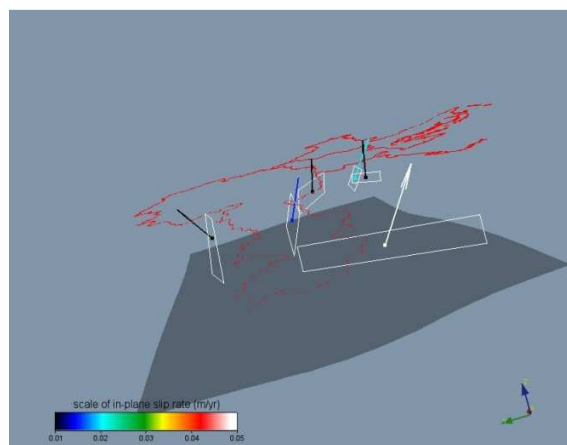

Fig. 5. Three dimensional view of our model, seen from West. The arrows indicate the direction of slip of the hanging wall relative to the footwall. On the Northern side (left) the geometry of the North Adriatic Thrust is visible, and the uplift of the Tauern window along a Sub-Tauern ramp, which is visible in seismic data. The red line represents the political borders of Austria, Slovenia, Italy and Croatia. The grey surface on the bottom gives a qualitative indication of a smoothed Moho, to indicate that the mapped rectangular faults are within the crust.

The nominal values of the rectangular faults in Table 1 are estimated with different uncertainties, primarily because of the uneven distribution of the velocity data. For example the large uncertainty in the slip rate of the Giudicarie stems from the presence of only one GPS station W of this structure, although the Eastern sector is well covered. Likewise the Montello and Friuli units, with their different strike angles, are necessary to split the velocity field just N of them into a NW and NE component.

The importance of each structural element can be defined in terms of the moment rate given in Table 2. The moment rate is the product of the potency rate (slip area x slip rate) and the shear modulus. The structural element in the Giudicarie area has the largest moment rate, as it involves a large active area and a large slip rate, although with a large uncertainty. However the seismicity is considerably smaller than in the Friuli-Montello region, where we introduced two different rectangular faults with different strike and rake. This suggests that seismic activity is more sensitive to the change of slip vector, rather than the size of the rectangular fault and absolute value of the slip at depth.
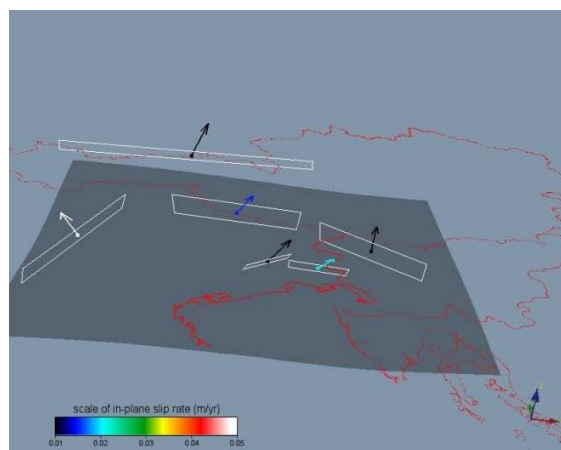

Fig. 6. The 3D model, seen from South.

The small size of the Friuli-Montello rectangles enables a steep decrease of the surface velocity moving North. There is no need to introduce a slip along the Pustertal Gailtal line, nor along the Schio Vicenza line. The flow is, North of the Pustertal Gailtal line, controlled by the transpressional

character of the Tauern and North Adriatic Thrust. Our model accounts for a lateral escape uniquely as a consequence of convergence and indentation. We have not attempted to include gravitational collapse and spreading as a driver for extrusion (Ratschbacher et al., 1991).
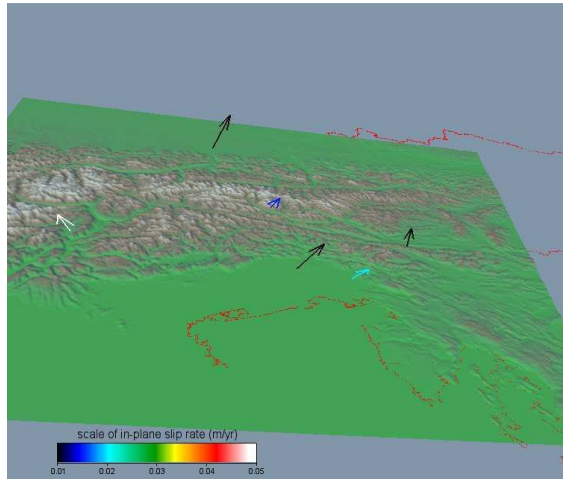

Fig. 7. Intersection of the in plane slip vectors with the topography (GTOPO30 model of NOAA).

With the exception of the Giudicarie and the North Adriatic Thrust (NAT), all the four remaining rectangular faults are reverse (Figure 7). The dips are moderate with the exception of the Giudicarie which shows a steep dip. The depths of the lowest left corners of the rectangles are variable, but remain within the thickened Alpine crust.

The highly seismic area of Friuli is associated with a rectangular fault of 45x25 km covering a depth range from 25 to 5 km and dipping at 55 deg.. This agrees with hypocenters being located around 10 km depth , on average, and with the fault plane solutions of the largest earthquakes. The potency (or moment) rate is smaller here than in other areas with less seismicity, suggesting that the moment rate is weekly correlated to seismicity. The large potency rate of the Giudicarie could be more in keeping with a regional stress drop which has recently been introduced on the basis of geodetic strain rates and regional Gutenberg-Richter parameters (Caporali et al., 2011).
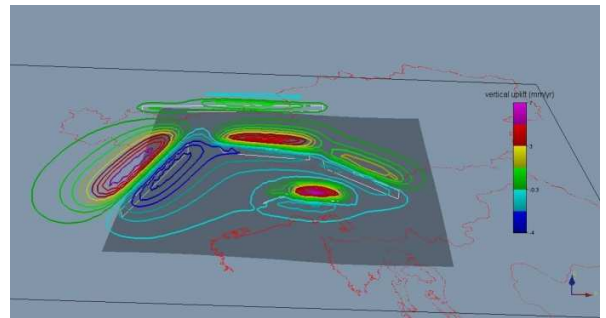

Fig. 8. Vertical rate according to the elastic model. A full scale model should include additional effects due to erosion and post glacial adjustment.

Vertical GPS velocities were not used to constrain the model, as they are insufficiently well determined in several cases. The model predicts vertical motion which is in qualitative agreement with independent data (Figure 8). In the Tauern window the uplift is measured to be of the order of 1 mm/yr (Hoeggerl, 2001) whereas our model predicts values as high as 4-5 mm/yr, with an uncertainty difficult to calculate, but which is likely to be of the order of few mm/yr. The model predicts likewise subsidence, e.g. in the NE of Italy (Po Plain) which would then add to other known effects. We emphasize that the vertical motions predicted by an elastic model need to be complemented with estimates of erosion rates, post glacial uplift and departures from elasticity, before they can be compared with data such as leveling, absolute gravity or GPS/DInSAR heighting.

4 Conclusion

The model presented here is intended to be a first attempt to describe in an area of active indentation the relationship between fault structure, seismology and surface kinematics. The deformation visible from GPS does not require an external horizontal stress (e.g. Nubia push) but can be modeled in terms of local structures. The rectangular faults which can be constrained by the available data resemble known structures. The model is able to discriminate which structure is undergoing to slip, so that further research can be stimulated on the relation between seismicity, slip at depth and surface flow. The structure with the largest slip at depth is the NW part of the indenter with a marked transcurrent rake angle. Yet seismicity concentrates

on the inner wedge (Friuli), where the slip area is smaller but the horizontal gradient is larger. The way in which stress is transferred from one rectangular fault to the neighbors is an important issue which awaits to be addressed.

Several areas are unfortunately still insufficiently constrained by the available GPS data, but it is only a matter of time to accumulate sufficiently long time series from existing and planned stations to fill the gaps in the velocity map. New preliminary data presented recently by the Slovenian group (Medved et al., 2011) indicate that the velocity pattern in the Upper Dinarids is very well in keeping with the pattern predicted by our model (Figure 4). DInSAR data are also expected to play a role, particularly on the vertical.

A final important remark is on the concept of convergence rate. For a rigid indenter the convergence rate near the margin is independent of depth. For a deformable margin, this is not the case, and larger velocities at depth are expected.

REFERENCES

Altamimi, Z., Collilieux, X., Legrand, J., Garayt, B., & Boucher, C., 2007. ITRF2005: A new release of the International Terrestrial Reference Frame based on time series of station positions and Earth Orientation Parameters. J. Geophys. Res., 112, B09401, doi:10.1029/2007JB004949.

Anderson, H., Jackson, J., 1987. Active tectonics of the Adriatic region. Geophys. J. R. Astron. Soc. 91, 937–983.

Barletta, V. R., Ferrari, C., Diolaiuti, G., Carnielli, T., Sabadini, R., Smiraglia, C. 2006. Glacier shrinkage and modeled uplift of the Alps, Geophys. Res.Lett., 33, L14307, doi:10.1029/2006GL026490.

Basili R., Valensise, G., Vannoli, P., Burrato, P., Fracassi, U., Mariano, S., Tiberti, M.M., Boschi, E., 2008. The Database of Individual Seismogenic Sources (DISS), version 3: summarizing 20 years of research on Italy's earthquake geology, Tectonophysics, doi:10.1016/j.tecto.2007.04.014

Battaglia, M., Murray, M.H., Serpelloni, E., Burgmann, R., 2004. The Adriatic region: an independent microplate within the Africa Eurasia collision zone. Geophys. Res. Lett., 1, L09605, doi: 10.1029/2004GL019723.

Bressan, G., Snidarcig, A., Venturini, C., 1998. Present state of tectonic stress of the Friuli Area (Eastern Southern Alps), Tectonophysics 292,211-227.

Brückl, E., Bleibinhaus, F., Gosar, A., Grad, M., Guterch, A., Hrubcovà, P., Randy Keller, G., Majdanski, M., Sumanovac, M., Tiira, T., Yliniemi, J., Hegedus, E., Thybo, H., 2007.Crustal structure due to collisional and escape tectonics in the Eastern Alps region based on profiles Alp01 and Alp02 from the ALP 2002 seismic experiment. J. Geophys. Res. 112, B06308. doi:10.1029/2006JB004687.

Brückl, E., Behm, M., Decker, K., Grad, M., Guterch, A., Keller, G. R., Thybo, H., 2010. Crustal structure and active tectonics in the Eastern Alps. TECTONICS, VOL. 29, TC2011, doi:10.1029/2009TC002491.

Caporali, A., 2003. Average strain rate in the Italian crust inferred from a permanent GPS network I. Statistical analysis of time series of permanent GPS stations. Geophysical Journal International, 155, 241-253.

Caporali, A., Braitenberg, C., Massironi, M., 2005. Geodetic and hydrological aspects of the Merano earthquake of 17 July 2001, J. of Geodyn. 39, 317 – 336, DOI: 10.1016/j.jog.2005.01.001.

Caporali, A., Aichhorn, C., Barlik, M., Becker, M.,Fejes, I., Gerhatova, L., Ghitau, D., Grenerczy, G.,Hefty, J., Krauss, S., Medak, D., Milev, G., Mojzes, M., Mulic, M., Nardo, A., Pesec, P., Rus, T., Simek, J., Sledzinski, J., Solaric, M., Stangl, G., Stopar, B., Vespe, F., Virag, G., 2009. Surface kinematics in the Alpine–Carpathian–Dinaric and Balkan region inferred from a new multi-network GPS combination solution Tectonophysics 474, 295–321doi:10.1016/j.tecto.2009.04.035

Caporali, A., Barba, S., Carafa, M.M., Devoti, R., Pietrantonio, G., Riguzzi F., 2011. Static stress drop as determined from geodetic strain rates and statistical seismicity. J. Geophys. Res., 116, B02410, doi:10.1029/2010JB007671.

Carulli, G.B., Nicolich, R., Rebez, A., Slejko, D., 1990. Seismotectonics of the Northwest External Dinarides.Tectonophysics 179, 11-25

Castellarin, A., Nicolich, R., Fantoni, R., Cantelli, L., Sella, M., Selli, L. 2006, Structure of the lithosphere beneath the Eastern Alps (southern sector of the TRANSALP transect), Tectonophysics,414(1–4), 259–282, doi:10.1016/j.tecto.2005.10.013.

CNR, Structural model of Italy, ed. by F. Barberi, SELCA editions, Firenze 1990.

Dach, R., Hugenthobler, U., Friedez P., Meindl M., 2007. Bernese GPS Software Version 5.0. Astronomical Institute, University of Bern, 612 pp.

D'Agostino, N., Cheloni, D., Mantenuto, S., Selvaggi, G., Michelini, A., Zuliani, D., 2005. Strain accumulation in the southern Alps (NE Italy) and deformation at the NorthEastern boundary of Adria observed by CGPS. Geophys. Res. Lett. 32, L19306, doi:10.1029/2005GL024266.

D'Agostino, N., A. Avallone, D. Cheloni, E. D'Anastasio, S. Mantenuto, G. Selvaggi, 2008. Active tectonics Adriatic region from GPS and earthquake slip vectors, J. Geophys. Res., 113, B12413, doi:10.1029/2008JB005860.

Gruppo di lavoro CPTI04, 2004. Catalogo paramentrico dei Terremoti Italiani, versione 2004 (CPTI04), INGV, Bologna ed. by P. Gasperini, R. Camassi, C. Mirto and M. Stucchi, (http://emidius.mi.ingv.it/CPTI04/)

Höggerl, N., 2001. Bestimmung von rezenten Höhenänderungen durch wiederholte geodätische Messungen, in Die Zentralanstalt für Meteorologie und Geodynamik 1851–2001, edited by C. Hammerl et al., 630–644, Leykam, Graz, Austria.

Linzer, H.-G., Decker, K., Peresson, H., Dell'Mour, R.,Frisch, W. 2002. Balancing lateral orogenic float of the Eastern Alps, Tectonophysics, 354 (3–4), 211–237, doi:10.1016/S0040-1951(02)00337-2.

Marton,E., Zampieri,D., Kazmer,M., Dunkl, I., Frisch,W., 2011. New Paleocene-Eocene paleomagnetic results from the foreland of the Southern Alps confirm decoupling of stable Adria from the African plate, Tectonophysics, 504, 89-99, DOI: 10.1016/j.tecto.2011.03.006.

Massironi, M., Zampieri, D. , Caporali, A., 2006. Miocene to present major fault linkages through the Adriatic indenter and the Austroalpine–Penninic collisional wedge (Alps of NE Italy), In MORATTI, G. & CHALOUAN, A. (eds): Tectonics of the Western Mediterranean and North Africa. Geological Society, London, Special Publications, 262, 245–258.

Neubauer, F., Fritz, H., Genser, J., Kurz, W., Nemes, F., Wallbrecher, E., Wang, X., Willingshofer, E., 2000. Structural evolution within an extruding wedge: model and application to the Alpine-Pannonian system, in: Urai, J., Lehner, F., and van Zee, W. (Eds.): Aspects of tectonic faulting (Festschrift in Honour of Georg Mandl), Springer, 141–153.

Okada, Y., 1985. Surface deformation due to shear and tensile faults in a half-space. Bull. Seismol. Soc. Am., 75, 1135-1154.

Pondrelli S., Salimbeni S., Morelli A., Ekström G., Postpischl L., Vannucci G. and Boschi E., European-Mediterranean Regional Centroid Moment Tensor Catalog: solutions for 2005-2008, *Phys. Earth Planet. Int.*, in press, 2011.

Ratschbacher, L., Frisch,W., Linzer, H.-G., Merle, O.,1991. Lateral extrusion in the Eastern Alps, part 2. Structural analysis. Tectonics 10, 257–271.

Regenauer-Lieb, K., Petit, J.P., 1997. Cutting of the European continental lithosphere; plasticity theory applied to the present Alpine collision. J. Geophys. Res. 102,7731–7746.

Schmid, S.M., Fuegenschuh, B., Kissling, E., Schuster, R., 2004. Tectonic map and overall architecture of the Alpine orogen. Eclogae Geol. Helv. 97, 93–117.

Schmid, S.M., Bernoulli, D., Fuegenscuh, B., Matenco, L., Schefer, S., Schuster, R., Tischler, M., Ustaszewski, K., 2008. The Alpine–Carpathian–Dinaric orogenic system: correlation and evolution of tectonic units. Swiss J. Geosci. 101, 139–183.

TRANSALP Working Group, 2002. First deep seismic reflection images of the Eastern Alps reveal giant crustal wedges and transcrustal ramps, Geophys.Res. L e t t . , 29(1 0) , 145 2 , doi :10. 1 0 29 /2002GL014911.

Weber, J., Vrabec, M., Stopar, B., Pavlovcic-Preseren, P., Dixon. T., 2006. The PIVO-2003 Experiment: A GPS Study of Istria Peninsula and Adria Microplate motion, and active tectonics in Slovenia, in The Adria Microplate: GPS Geodesy, Tectonics and Hazards, NATO Sci. Ser. IV, vol. 61, edited by N. Pinter et al., pp. 321–334, Springer, New York.